Control of metal dispersion and structure by changes in the solid-state chemistry of supported cobalt Fischer–Tropsch catalysts

Stuart L. Soled[a,*], Enrique Iglesia[a,b], Rocco A. Fiato[a], Joseph E. Baumgartner[a], Hilda Vroman[a], and Sabato Miseo[a]

[a] *ExxonMobil Research and Engineering Company, Annandale, NJ, USA*
[b] *Department of Chemical Engineering, University of California at Berkeley, Berkeley, California, USA*

Controlling preparation variables in supported cobalt Fischer–Tropsch catalysts has a dramatic effect on the dispersion and distribution of cobalt, and determines how active and selective the resulting catalyst will be. We detail specific examples of catalyst synthesis strategies for modifying interactions between the support and the cobalt precursor, promoting reduction, stabilizing catalysts to high-temperature treatments, minimizing deleterious support metal interactions, and controlling the distribution of cobalt on large support particles. It is important to optimize the support and precursor interaction strength, so that it is strong enough to obtain good dispersion but not too strong to prevent low temperature reduction. We show examples in which formation of surface complexes and epitaxial matching of precursor and support structures improves dispersion dramatically. Reduction promoters can help in those cases where support–precursor interactions are too strong. We show how substitutions of silicon into a titania lattice stabilizes surface area and retards formation at high oxidation temperatures of cobalt ternary oxides that reduce only at very high temperatures—an important consideration if oxidative coke removal is necessary. In addition, surface treatment of TiO_2 with an irreducible oxide like ZrO_2 can inhibit deleterious support interactions that can block surface cobalt sites. Selectivity can also be dramatically altered by catalyst synthesis. We illustrate a case of large (2 mm) SiO_2 particles onto which cobalt can be added either uniformly or in discrete eggshells, with the eggshell catalysts having substantially higher C_{5+} selectivity. These approaches can lead to optimal Fischer–Tropsch catalysts with high activity and C_{5+} selectivity, good physical integrity, and a long life.

KEY WORDS: supported cobalt catalysts; Fischer–Tropsch synthesis; catalyst preparation cobalt dispersion.

1. Introduction

Fischer–Tropsch (FT) synthesis catalysis has seen a renewed interest during the last two decades, but important catalytic chemistry and engineering issues remain in the search for catalyst systems with higher activity and C_{5+} selectivity [1–5]. Most recent efforts have focused on supported cobalt instead of iron catalysts because their low water–gas shift activity minimizes the consumption of carbon in oxygen rejection steps and leads to higher thermal and carbon efficiencies. Previous studies have shown the importance of controlling the dispersion, extent of reduction, location, and density of cobalt species [6–8] in order to achieve these desired properties. Here, we primarily focus on understanding how catalyst synthesis variables such as cobalt precursors, supports, pretreatment methods, site densities, and bimetallic promoters affect cobalt dispersion and Fischer–Tropsch rates and selectivity. We illustrate the importance of balancing support–precursor interactions so that they are strong enough to disperse the precursor but not too strong to require high temperature reductions that will sinter cobalt crystallites. Supports can also deleteriously affect the cobalt by decorating its surface or forming mixed oxides that do not reduce. We illustrate some examples where we have overcome these issues. Controlling cobalt placement in large support particles can have an important influence on the C_{5+} selectivity and we describe a synthesis procedure that allows us to control this morphology. In this paper, we attempt to show rational design strategies for preparing an active, selective, and stable Fischer–Tropsch catalyst.

To whom correspondence should be addressed.

2. Experimental

2.1. Sample preparation

Table 1 summarizes the different sample preparations described in this section.

Co/SiO_2 (20 wt%) was prepared by incipient wetness impregnation with a cobalt nitrate solution (prepared from cobalt nitrate hexahydrate, Alfa, Puratronic grade) onto Davison 62 silica (280 m^2/g; sample a). In a parallel preparation, another Co/SiO_2 was prepared using a cobalt nitrate-impregnating solution containing four moles of citric acid (Aldrich, 99.5%) per gram atom cobalt (sample b). After impregnation, samples were dried at 120 °C and then heated at 450 °C for 4 h in ambient air. Ruthenium (0.3 wt%) was added to a portion of the calcined Co/SiO_2 sample (sample b) by immersing 20 g of the sample into a 100 cc acetone

1022-5528/03/1200–0101/0 © 2003 Plenum Publishing Corporation

Table 1
Sample matrix

Sample #	Support	Cobalt loading (%)	Other metal	Preparation technique
a	Davison 62 silica	20		Cobalt nitrate i.w.
b	Davison 62 silica	20		Cobalt nitrate/citric acid i.w.
c	Davison 62 silica	20	0.3% ruthenium	Cobalt nitrate/citric acid i.w.
d	2.2 mm silica spheres	13		Cobalt nitrate melt limited c.t.
d′	2.2 mm silica spheres	13		Sample d calcined
e	Ground 2.2 mm silica spheres	13		Cobalt nitrate melt limited c.t.
f	2.2 mm silica spheres	13		Cobalt nitrate i.w.
g	Ground 2.2 mm silica spheres	13		Cobalt nitrate i.w.
h	$MgCr_2O_4$	12		Cobalt nitrate i.w
i	$MgCr_2O_4$	12	0.3% ruthenium	Cobalt nitrate i.w; ruthenium nitrate slurry dry
j	Davison 62 silica	20		Cobalt carbonyl
k	$1\%ZrO_2/TiO_2$ ($15\,m^2/g$, zirconium surface treat)	11	1.0% rhenium	Cobalt nitrate, perrhenic acid i.w.
l	TiO_2 ($15\,m^2/g$)	11	1.0% rhenium	Cobalt nitrate, perrhenic acid i.w.
m	$Ti_{2-x}Si_xO_2$ ($0.14 \geq x \geq 0$)	none		
n	$Ti_{2-x}Zr_xO_2$ ($0.14 \geq x \geq 0$)	none		
0	$Ti_{-0.86}Si_{0.14}$	12		Cobalt nitrate i.w.
p	TiO_2 (from titanium *tert*-butoxide hydrolysis)	12		Cobalt nitrate i.w.

Note: i.w. = incipient wetness; c.t. = contact time.

solution containing ruthenium nitrate (Engelhard Corporation), and then allowing the excess solution to evaporate while stirring the slurry. After drying at 120 °C, the sample was heated at 350 °C for 4 h in ambient air (sample c).

Another Co/SiO_2 (13 wt%) sample was prepared by pouring cobalt nitrate melts (~75 °C) over a 2–3 cm stirred bed of 2-mm SiO_2 spheres (Shell S980G, $115\,m^2/g$, 99.9%). The spheres were placed in a vacuum funnel in order to limit their contact time with the molten cobalt nitrate for 2–4 s. This technique produced a well-defined ~100μ eggshell ring (sample d). Reductions were carried out in flowing pure H_2 on either the as-prepared nitrate melts or after treating these nitrate-impregnated samples in ambient air at 350 °C for 4 h in order to form cobalt oxide (sample d′). Heating rates were varied from 0.2 to 4 °C/min during the reduction process. A fraction of the eggshell spheres (not calcined) were ground and sieved to form small particles (~0.17 mm diameter, sample e). In addition, we prepared an evenly impregnated sample of 13 wt% cobalt on the same 2.2 mm spheres by an incipient impregnation of an aqueous cobalt nitrate solution. This sample was dried overnight at 120 °C and calcined for 4 h at 350 °C in ambient air (sample f). A fraction of these spheres were also crushed to 0.17 mm diameter (sample g).

$MgCr_2O_4$ was prepared by adding a solution containing glycolic acid and ammonium hydroxide at a pH of 6.5 to a separate solution containing magnesium and chromium nitrates, such that the number of moles of glycolic acid equals the combined number of moles of magnesium and chromium. The resulting mixture was allowed to dry at ambient conditions for several days. The glassy amorphous material that formed during this time was then heated in ambient air at 350 °C for 4 h. This procedure led to the formation of monophasic high surface area $MgCr_2O_4$ powders with a spinel structure. Cobalt was impregnated onto the support to give a cobalt content of 12 wt% using an aqueous cobalt nitrate solution (Alfa, Puratronic). The impregnated sample was dried and heated at 350 °C in ambient air (sample h) and 0.3 wt% ruthenium was added onto a portion of it and this catalyst was calcined at 350 °C in ambient air (forming sample i).

A 20 wt% Co/SiO_2 sample was prepared using dicobalt octacarbonyl ($Co_2(CO)_8$) dissolved in degassed acetone (Aldrich, spectroscopic grade). This solution was contacted with SiO_2 (Davison 62) under N_2 and the resulting slurry was stirred at ambient temperature for 1 h. The acetone was removed under vacuum at ambient temperature, and the sample decarbonylated under vacuum at 120 °C and then passivated in 1% O_2/Ar at room temperature before exposure to ambient air (sample j).

A sample of 1 wt% ZrO_2/TiO_2 was prepared by incipient wetness impregnation of a solution of $ZrO(NO_3)_2$ (Alfa) onto a support of $\sim 15\,m^2/g$ surface area (~85% rutile, 15% anatase, Degussa P25 calcined at 850 °C for 1.5 h). The sample was dried at 120 °C overnight and heated at 400 °C for 4 h in ambient air. The sample was impregnated with a solution of cobalt nitrate (Alfa, Puratronic grade) and perrhenic acid (Alfa) to give 11 wt% cobalt and 1 wt% rhenium. This sample was dried at 120 °C overnight and heated in ambient air at 350 °C for 4 h (sample k). A second sample was prepared in an analogous manner but without zirconia impregnation (sample l).

Titania-silica and titania-zirconia mixed oxides with up to 14 mol% silicon or zirconium substituted for

titanium in the lattice were prepared by hydrolysis of mixtures of titanium *tert*-butoxide with either tetramethyl-orthosilicate or zirconium *n*-propoxide at ambient temperature using four H_2O molecules per total metal atom in the alkoxide mixture [9]. The solids were dried at 120 °C overnight and heated at 700 °C in ambient air for 4 h (sample series m and n). Cobalt (12 wt%) was deposited on the sample of $Ti_{.86}Si_{.14}O_2$ that had been calcined at 700 °C as well as on a 350 °C calcined sample of neat TiO_2 prepared from the sol–gel synthesis. These impregnations were carried out using aqueous, incipient wetness, and the samples dried and heated in ambient air to 350 °C for 4 h (samples o and p). A portion of these samples was also heated at temperatures between 650 and 900 °C for 4 h and examined by X-ray diffraction (Cu K_α radiation). The relative amounts of anatase, rutile, and cobalt titanate in the high-temperature heated samples were estimated from the integrated intensities of the X-ray diffraction peaks with *d* values between 1.5 and 7.5 Å. For calibration, a known weight of each individual phase was separately measured.

2.2. Chemisorption

H_2 chemisorption uptakes on a manual glass adsorption rack using single adsorption isotherm methods were measured volumetrically on the catalysts shown in figures 1, 4, and 5 at 100 °C using the total H_2 uptake and a 1:1 H:Co adsorption stoichiometry [10]. The chemisorption data shown in figure 8 were measured using an automated volumetric apparatus (Quantachrome Autosorb 1C) to obtain the difference between the total and the weakly held hydrogen at 40 °C, also using a 1:1 H:Co stoichiometry [11]. In order to minimize SMSI effects on chemisorption uptakes, the Co-loaded TiO_2 catalyst in figure 8 was reduced *ex situ* in flowing H_2 at 1 atm by heating the samples to 375 °C at 4 °C/min and holding for 2 h. The sample was then cooled to ambient temperature, passivated by exposure to a 0.5% O_2 stream, and treated at 150 °C in flowing dry air, before re-reduction at 225 °C before H_2 chemisorption measurements. Treatment in air at 150 °C removes the SMSI "overlayer" formed during the initial reduction at 375 °C and renders the sample reducible at lower temperatures, where overlayer formation is minimal [12]. After these passivated samples were re-reduced at 225 °C in 1 atm flowing H_2, any chemisorbed hydrogen was removed by evacuation at this temperature for 0.75 h, and H_2 chemisorption uptakes measured at 10–55 kPa H_2 pressure and 40 °C. The weakly held fraction of this adsorbed hydrogen was measured by evacuating the sample at 40 °C after H_2 adsorption and measuring a subsequent adsorption isotherm. Long equilibration times (up to 1 h) were used in order to ensure adsorption–desorption equilibrium. Even at 225 °C, H_2 treatments can lead to TiO_{2-x} overlayers. In order to determine if any overlayer effects influenced the measured uptakes, we also examined the effect of reduction times (at 225 °C reduction temperature) on H_2 chemisorption uptakes. Cobalt dispersions are reported as the H/Co ratio obtained from the H_2 uptakes and the cobalt content was measured by ICP analysis.

2.3. Catalytic evaluation

Fischer–Tropsch rates and selectivities were measured in a packed-bed reactor as described previously [6]. Fischer–Tropsch synthesis rates were measured at 200 °C, H_2/CO ratios of 2:1, pressures of 2000 kPa, and CO conversions of 50–60%.

3. Results and discussion

3.1. Precursor, support, and bimetallic effects

In previous studies, Fischer–Tropsch synthesis rates per surface cobalt atom site were shown to depend only weakly on the identity of the support and on the size of the Co crystallites, at least for crystallites larger than ~8 nm (figure 1) [6]. The synthesis of cobalt metal particles smaller than 15 nm usually requires the reduction of a well-dispersed precursor or an intermediate. Cobalt oxide is the most common intermediate formed after heating of nitrate or other precursors. Cobalt oxides form well-dispersed surface crystallites only when they interact strongly with the oxide support. Strongly interacting cobalt oxide crystallites, however, are more difficult to reduce than corresponding bulk cobalt oxides, and the high reduction temperatures required to form the active metal phase lead to poor metal dispersion. In contrast, weakly interacting supports lead to poor dispersion of the cobalt oxide intermediates, which reduce at relatively low temperatures but form correspondingly large cobalt metal crystallites. As a result, a balance between the dispersion

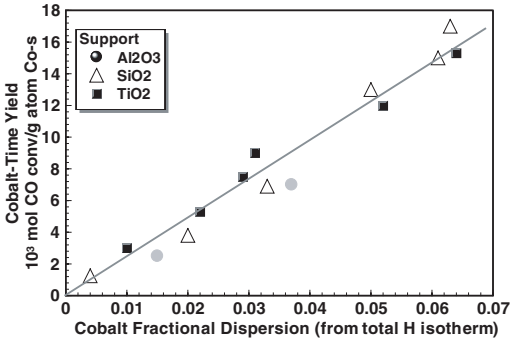

Figure 1. Cobalt time yields for a variety of silica, alumina and titania catalysts. Dispersion measured from single adsorption isotherm at 100 °C [3] on fresh reduced catalysts. Fischer–Tropsch synthesis at 200 °C, $H_2/CO = 2:1$, 2000 kPa, 50–60% CO conversion.

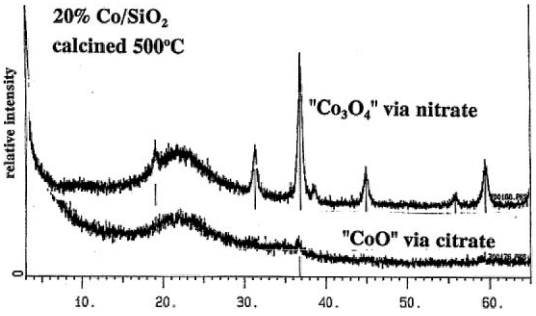

Figure 2. X-ray diffraction patterns for heated 20 wt% Co/SiO_2 samples prepared by nitrate (sample a) or nitrate–citric acid impregnation methods (sample b).

of the cobalt oxide intermediates and their reducibility, achieved through changes in the support and the precursor, is required for optimum cobalt metal dispersion.

These trends are illustrated in figure 2, where the X-ray diffraction patterns are shown for 20 wt% Co/SiO_2 samples prepared by heating of nitrate and of nitrate/citric acid precursors (samples a and b). Co_3O_4 is clearly visible for the sample prepared from a nitrate precursor, but no crystalline cobalt oxide or oxyhydroxide are observed for the sample prepared with a nitrate/citric acid impregnating solution. The cobalt–citrate complex apparently forms a strongly interacting surface phase with the silica that converts into a well-dispersed oxide phase after calcination.

The resulting materials also show significantly different reduction dynamics during subsequent treatment in H_2. The larger Co_3O_4 crystallites prepared from nitrate precursors reduce to cobalt metal at ~250 °C, while the dispersed oxide species formed from the nitrate–citric acid precursors start reducing only at ~600 °C (figure 3). Figure 3 also shows the effect of adding 0.3 wt% ruthenium as a reduction promoter to samples with a strongly interacting dispersed cobalt oxide phase (sample c). The onset of reduction of this phase to cobalt metal occurs at 200–300 °C lower temperatures when very small amounts of ruthenium are present (Ru/Co = 1/115 atomic ratio). These lower reduction temperatures inhibit sintering. A cobalt dispersion of 5.4% (~10% on a reduced cobalt basis) was measured on the cobalt–ruthenium sample after reduction at 500 °C for 4 h, while H_2 uptakes were not detectable on the monometallic sample after the same treatment. The easily reduced Co/SiO_2 sample prepared from nitrate precursors showed a dispersion of 3.1% after complete reduction at 300 °C for 4 h. This example shows that the poorly dispersed oxide, although easily reducible, has a low dispersion, whereas the fully dispersed oxide cannot be reduced and therefore shows no H_2 chemisorption uptake. Adding a reduction promoter to the well-dispersed sample leads to the highest dispersion among these samples.

A good dispersion of cobalt oxide precursors was also achieved by epitaxially matching the structures of the support and of the supported cobalt oxide in an attempt to increase oxide-support interactions. $MgCr_2O_4$, with a surface area of 95 m^2/g, was prepared and used as a support for Co_3O_4. $MgCr_2O_4$ adopts a spinel structure similar to that of Co_3O_4 with a unit cell parameter of 8.33 Å, compared to a value of 8.08 Å for Co_3O_4. Cobalt

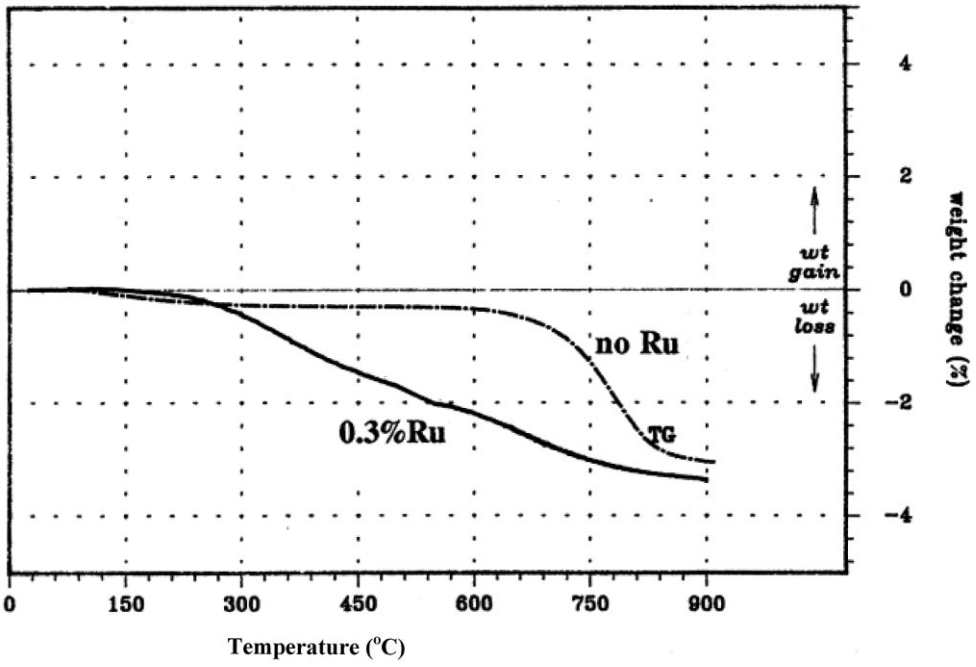

Figure 3. Thermogravimetric measurements of the extent of reduction for 20 wt% Co/SiO_2 samples prepared from nitrate–citric acid precursors with and without added ruthenium (0.3 wt%) (sample b versus sample c). Samples were heated at 4 °/min in 100% H_2 flow. 50 mg of sample was treated with 50 cc/min H_2 flow.

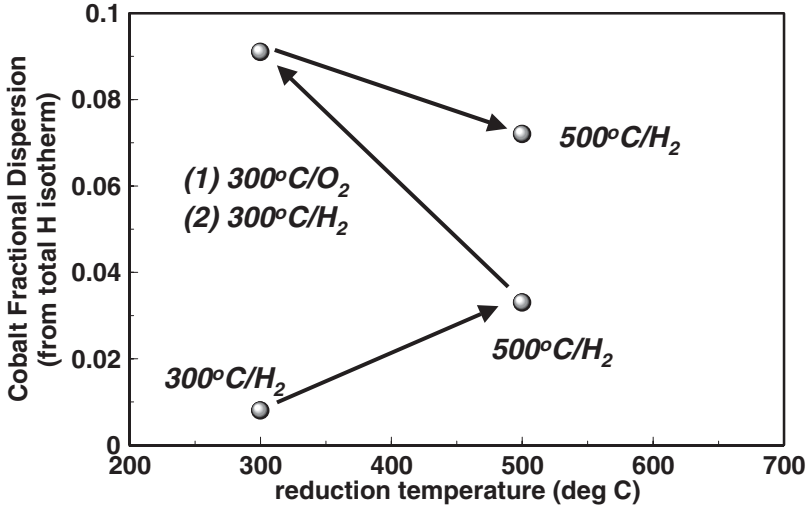

Figure 4. Cobalt dispersions measured from H_2 chemisorption [3] on 12 wt% cobalt, 0.3 wt% ruthenium on $MgCr_2O_4$ (sample i) as a function of reduction–oxidation treatments.

oxide prepared from nitrate precursors supported on $MgCr_2O_4$ reduces incompletely by 500 °C (sample h); therefore, ruthenium was added as a reduction promoter (sample i). Figure 4 shows the cobalt metal dispersion measured from H_2 chemisorption for sample (i) as a function of the sample treatment. Reduction at 300 °C gives H/Co ratios of less than 1% because of the inability to reduce cobalt completely. After reduction in H_2 at 500 °C, the cobalt metal dispersion (on the basis of the total cobalt) was 3.8%. After passivation at ambient temperature in a 1% O_2/Ar stream, the sample was treated in flowing dry air at 300 °C for 4 h. A subsequent treatment in H_2 at 300 °C for 4 h now shows a marked increase in cobalt dispersion to 9.2%, a value that slightly decreased to 7.2% after a subsequent treatment in H_2 at 500 °C for 4 h. Thermogravimetric studies confirmed that the rate and extent of reduction was dramatically enhanced for the sample first reduced at 500 °C and then reoxidized at 300 °C compared with the initial oxide sample formed by treating the nitrate precursors in air. Thus, it appears that oxidation treatments of prereduced Co–Ru catalysts decrease the required reduction temperatures and increase cobalt dispersion. Similar effects of reduction–oxidation–reduction cycles on reducibility were first reported for Co-Ru/La_2O_3/Al_2O_3 catalysts [13]. These cycling effects appear to reflect the mixing of cobalt and ruthenium to form stable $Co_{3-x}Ru_xO_4$ mixed solid solutions from initially prepared samples containing predominately separate cobalt and ruthenium oxide phases. After the bimetallic mixing occurs during cycling, reduction occurs faster than for the separate phases, apparently as a result of the ability of RuO_x species to initiate reduction within a Co-rich oxide phase. Our previous studies of Co-Ru/TiO_2 and Ru-doped cobalt foils [14] confirm the tendency of cobalt and ruthenium to form mixed oxides at ~300 °C oxidation and the effect of ruthenium to increase the rate of reduction of cobalt oxides.

The supported catalyst with the smallest cobalt crystallites on SiO_2 supports was prepared via decomposition of cobalt carbonyl (sample j). We detect cobalt metal particles with average diameter ~3 nm by transmission electron microscopy. These samples, however, showed Fischer–Tropsch cobalt-time yields significantly lower than the predicted data shown in figure 1. These results appear to reflect the tendency of very small monometallic cobalt crystallites to oxidize during Fischer–Tropsch reactions, which produce water as a by-product of hydrocarbon formation [15]. Similar low site activities have been reported for other cobalt carbonyl preparations in the literature [16].

3.2. Pretreatment effects

The ultimate dispersion of cobalt metal crystallites also depends on the procedures used to decompose or reduce the precursor. The heating rate during the conversion of the cobalt precursor or intermediate to cobalt metal and the identity of the precursor or intermediate (e.g. nitrate versus oxide) influence the concentrations of H_2O, NH_3, and NO_x products and may also influence the severity of local exotherms caused by decomposition or reduction reactions. Figure 5 compares the effect of heating rate during the reduction of cobalt nitrate precursors, without intervening treatment in air to form Co_3O_4 intermediates, with that of the oxidized nitrate (sample d versus d′). The reduction of nitrate-derived CoO_x species by raising the temperature to 350 °C at 4 °C/min gave a sample with a cobalt dispersion of 3.3%, while a similar reduction procedure, but without the intervening conversion of cobalt nitrate to cobalt oxides, led to significantly higher cobalt dispersions (6.2%). A slower temperature ramp

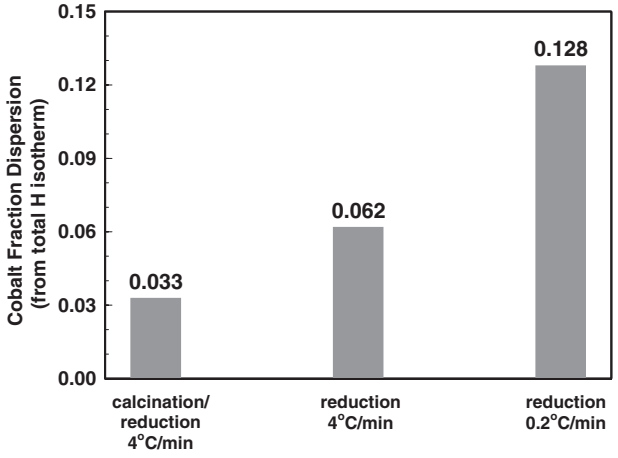

Figure 5. Cobalt dispersions following reduction of 13 wt%. cobalt supported on SiO_2 catalysts prepared on 2 mm silica spheres. The heated/reduced sample represents the supported oxide (sample d′), whereas the other two samples are directly reduced from the impregnated nitrate (sample d). Dispersions measured at 100 °C by the single isotherm method [3].

(0.2 °C/ min) during nitrate decomposition and reduction tends to decrease local exotherms and H_2O, NH_3, and NO_x product concentrations and leads to even higher dispersions (12.8%). The latter dispersion value corresponds to cobalt crystallites with ~7–8 nm diameter.

3.3. Thermal stability

So far, we have discussed approaches to control the dispersion of cobalt in supported catalysts through changes in the support and preparation variables. Other Fischer–Tropsch process considerations may introduce the need for other catalyst modifications. One requirement is that catalysts and supports retain their surface area and structure during high-temperature oxidative regeneration treatments. The requisite high-temperature oxidative treatments can lead to support sintering and to the formation of irreducible cobalt-containing mixed oxides. Next, we describe the synthesis and use of thermally stable supports for Co-based Fischer–Tropsch synthesis catalysts.

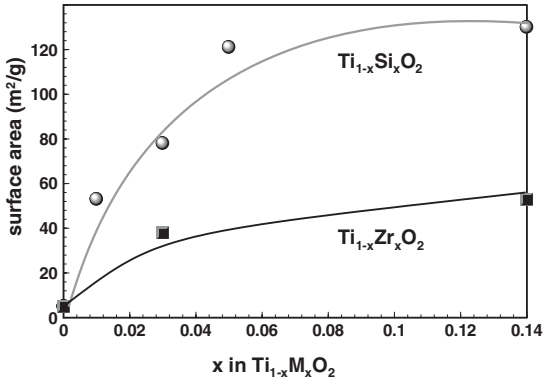

Figure 6. N_2 BET surface areas for titania with silicon and zirconium lattice substitutions after heating in air at 700 °C as a function of the concentration of silicon or zirconium (sample series m and n).

The substitution of silicon or zirconium atoms into the TiO_2 lattice inhibits loss of surface area during high-temperature thermal treatments [9,17] and retards the formation of irreducible cobalt titanate phases. Figure 6 shows that these substitutions (up to Zr/Ti and Si/Ti atomic ratios of 0.14) led to significantly higher surface areas than for pure TiO_2 after heating in ambient air at 700 °C for 4 h. For example, a $Ti_{0.95}Si_{0.05}O_2$ sample maintained a surface area of 120 m^2/g and retained the anatase crystal structure after treatment at 700 °C, while pure TiO_2 converted to the rutile structure with a concurrent decrease in surface area to 5 m^2/g. Silicon and zirconium substitutions have the additional benefit of preventing the formation of CoO-TiO_2 bulk compounds during these oxidative treatments. For the 12 wt% Co-containing samples, a cobalt titanate phase is first detected on pure TiO_2 supports after heating at 650 °C (sample p). On $Ti_{0.86}Si_{0.14}O_2$, this phase is detected only above 750 °C (sample o). Figure 7 shows the fraction of cobalt titanate in the presence of anatase and rutile as a function of calcination temperature for these two samples. These data indicate that the substitution of silicon into the titania lattice inhibits the formation of cobalt titanate phases. These cobalt titanate structures do not reduce during subsequent H_2 treatments; as a result, the formation of these bulk compounds removes cobalt atoms from the active cobalt metal pool required for Fischer–Tropsch synthesis reactions. The substitution of silicon into titania provides a mechanism for increasing catalyst stability at high temperatures. Although, we did not measure these inhibition effects for zirconium modifications, we expect similar behavior.

3.4. Strong metal-support interactions

In addition to the improvements in thermal stability illustrated above, support modifications can also be used in order to eliminate deleterious metal-support effects, such as the formation of TiO_{2-x} monolayers on metal crystallites. Some specific concerns about these SMSI effects have arisen in Co/TiO_2 Fischer–Tropsch catalysts [4]. The decoration of metal particles by reducible oxide species, such as TiO_{2-x}, during H_2 treatment at elevated temperatures can lead to the blockage of surface cobalt atoms during prereduction or even at the reducing conditions present within many Fischer–Tropsch reactors [18]. H_2 uptakes during chemisorption measurements are typically used to diagnose these decoration effects as well as the removal of these decorating layers by mild oxidative treatments. These experiments were carried out in order to examine the feasibility of eliminating decoration effects by modifying the surface of TiO_2 with an irreducible oxide. We report strong H_2 chemisorption uptakes at

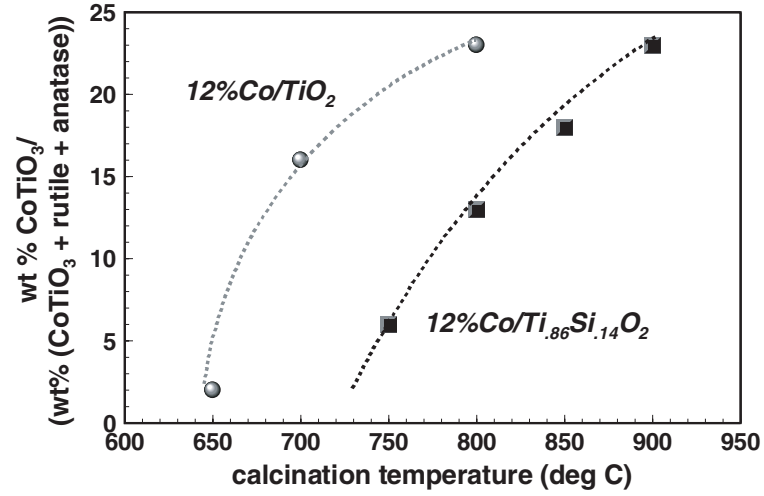

Figure 7. Percent of titania involved in $CoTiO_3$ formation on calcining 12 wt% cobalt supported on TiO_2 (sample p) and $Ti_{0.86}Si_{0.14}O_2$ (sample o) at increasing temperatures.

40 °C on identically prepared Co-Re (11%/1%) samples supported on TiO_2 and on the same TiO_2 but surface-modified with 1 wt% ZrO_2 (samples l and k). For both materials, all of the cobalt precursors were reduced to cobalt metal before H_2 chemisorption measurements.

Figure 8 shows the decrease in strongly adsorbed hydrogen typical of SMSI effects as a function of reduction time at 225 °C for Co-Re/TiO_2 and the corresponding nearly constant H_2 uptake values for Co-Re/ZrO_2-TiO_2. Both samples were initially treated in H_2 at 375 °C for 2 h in order to reduce all Co_3O_4 precursors to cobalt metal and then passivated in a 0.5% O_2 stream at ambient temperature. The samples were then heated slowly (2 °C/min) in air to 150 °C in air and held at 150 °C for 2 h in order to reverse any decoration effects caused by the initial reduction at 375 °C. After these procedures, the samples were reduced in pure H_2 at 225 °C for various periods of time in order to generate the data shown in figure 8. In these experiments, we are observing reduction of both cobalt and titania. Cobalt reduction increases the chemisorption uptakes until the cobalt becomes fully reduced, whereas titania reduction decreases the chemisorption uptakes. The initial chemisorption value (4.2%) on Co-Re/TiO_2 is substantially higher than that measured immediately after reduction at 375 °C for 2 h (2.6%) without air treatment, consistent with more severe decoration effects at these higher reduction temperatures. This sample appears to be fully reduced after the first (90 min) reduction point. On the ZrO_2-treated TiO_2 support, H_2 treatments up to 30 h at 225 °C did not significantly decrease H_2 uptakes, indicating that modifications of TiO_2 surfaces with ZrO_2 inhibit the decoration of cobalt metal particles during reduction at 225 °C. In this ZrO_2-modified

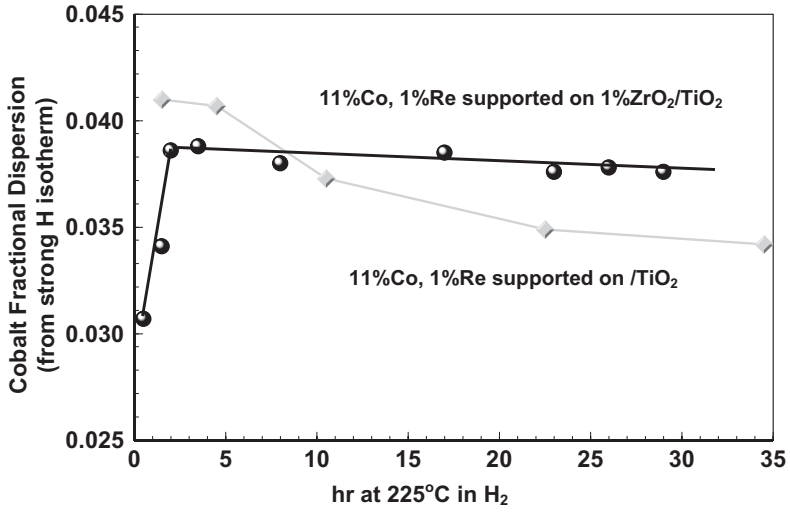

Figure 8. Comparison of strong hydrogen chemisorption values on 11 wt% cobalt and 1 wt% rhenium supported on titania and 1% ZrO_2/TiO_2 (samples l and k respectively) following successive reductions at 225 °C. Both samples were initially treated in H_2 at 375 °C for 2 h in order to reduce all Co_3O_4 precursors to cobalt metal and then passivated in a 0.5% O_2 stream at room temperature. They were then slowly (2 °C/min) oxidized to 150 °C in air and held at that temperature for 2 before being reduced at 225 °C for the times indicated in the figure.

Table 2
Strong H_2 chemisorption measurements for 11 wt% cobalt and 1 wt% rhenium supported on titania and 1% ZrO_2/TiO_2 (samples l and k respectively). Combined and backsorption isotherms measured at 40 °C. Reductions were carried out in flowing hydrogen at 1 atmosphere pressure

Pretreatment	Reduction	11% cobalt, 1% Re/TiO_2	11% cobalt, 1% $Re/1\%ZrO_2/TiO_2$
Reduce 375 °C/oxidize 150 °C	Reduce 225 °C (1.5–2 h)	4.16	3.86
	Reduce 375 °C (2 h)	2.55	3.89
	Reduce 375 °C (2 h)–450 °C (2 h)	1.91	2.67
Ratio chemisorption 375 °C/225 °C		0.61	1.0
Ratio chemisorption 450 °C/225 °C		0.46	0.69

sample, the cobalt was not fully reduced at 225 °C until after 3 h reduction. Table 2 shows that decoration effects can be detected after reduction at higher temperatures, but these effects are much weaker for ZrO_2-modified TiO_2 surfaces than for pure TiO_2 surfaces.

3.5. Transport effects

The findings presented above demonstrate that some control over cobalt dispersion, stability of the support, and the tendency of certain supports to form bulk or surface compounds with cobalt metal or oxide crystallites can be achieved by changes in synthetic protocols and precursors and by modification of the support. All of these catalyst properties influence the activity and stability of cobalt-based Fischer–Tropsch synthesis catalysts. The modifications in catalyst supports, precursor, and preparation techniques can also influence Fischer–Tropsch selectivity. For example, intermediate levels of transport restrictions in large diameter support particles, achieved by controlling the density and location of cobalt sites and the pore structures of supports, can have a beneficial effect on selectivity [19]. Maximizing C_5^+ and minimizing CH_4 selectivity requires careful consideration of the number and location of active sites within complex support pore structures.

In preparing selective large particle catalysts, we utilized a technique that limits diffusion times of high viscosity cobalt nitrate melts into the pores of 2-mm silica spheres. We coupled this preparation procedure with the direct reduction of the nitrate melts without prior oxidation in order to obtain some of the highest reported dispersions of cobalt metal at very high local cobalt contents and site densities. By combining the two techniques, ~100 μm cobalt eggshells containing crystallites smaller than 10 nm at local cobalt contents of ~50% were achieved (sample d). The location and active site density provided an intermediate level of transport restrictions that promoted olefin adsorption and chain growth, without introducing CO concentration gradients, which favor CH_4 production. Table 3 compares Fischer–Tropsch selectivity data on 13% cobalt catalysts on the same 2.2-mm silica spheres prepared in a uniform distribution (sample f) with those obtained on similar spheres but with a 100 μm eggshell (sample d). Ground versions of each of these catalysts were also evaluated (samples e and g). Note that the preparation of the eggshell dramatically decreases methane and increases C_{5+} compared to the uniformly impregnated pellet. This difference in selectivity is attributed to transport-induced CO gradients in the uniform pellets that create higher effective H_2/CO ratios in the interior of the particle. Furthermore, the ground eggshell pellets give higher C_{5+} selectivity than the ground uniform pellets with the same (small) size. This illustrates the impact of inducing moderate transport restrictions and of achieving high cobalt dispersions at very high local cobalt loadings on Fischer–Tropsch synthesis rates and C_{5+} selectivities.

4. Conclusions

Control of support/surface interactions is a key parameter for obtaining optimum dispersions, reducibility, and metal distribution in Fischer–Tropsch synthesis

Table 3
Selectivities for 2-mm diameter $13\%Co/SiO_2$ catalysts, silica surface area 115 m^2/g; Fischer–Tropsch reaction at 200 °C, 2000 kPa, $H_2/CO = 2.1$, 55–65% conversion, > 24 h onstream

	Uniformly impregnated pellets (sample f)	Crushed uniform pellets (sample g)	Eggshell pellets (sample d)	Crushed eggshell pellets (sample e)
Pellet diameter (mm)	2.2	0.17	2.2	0.17
Average thickness of impregnated region (mm)	2.2	0.17	0.23	0.17
H/Co chemisorption (percent dispersion) [3]	3.3%	3.3%	12.8%	12.8%
CH_4 selectivity	12.1	5.2	7.7	4.7
C_{5+} selectivity	81.5	89.6	88.0	90.5

catalysts. We illustrate several successful examples of improvements in cobalt dispersion achieved by changing synthetic parameters as well as stabilizing catalysts to high-temperature treatments or avoiding SMSI effects. The design of Fischer–Tropsch catalysts to ensure optimum activity, selectivity, strength, and life continues to provide significant challenges.

References

[1] M.E. Dry, Appl. Catal., A 138 (1996) 319.
[2] E. Iglesia, Appl. Catal., A 161 (1997) 59.
[3] C.H. Bartholomew, Stud. Surf. Sci. Catal. 64 (1991) 158.
[4] R. Oukaci, A.H. Singleton and J.G. Goodwin, Appl. Catal., A 186 (1999) 129.
[5] S.C. Saxena, Catal. Rev.—Sci. Eng. 37(2) (1995) 227.
[6] E. Iglesia, S.L. Soled and R.A. Fiato, J. Catal. 137 (1992) 212.
[7] E. Iglesia, S.C. Reyes, R.J. Madon and S.L. Soled, Adv. Catal. 39 (1993) 221.
[8] A. Barbier, A. Tuel, I. Arcon, A. Kodre and G.A. Martin, J. Catal. 200 (2001) 106.
[9] S. Soled and G.B. McVicker, Prepr.—Am. Chem. Soc., Div. Pet. Chem. 34 (1989) 645.
[10] R.C. Reuel and C.H. Bartholomew, J. Catal. 85(1) (1984) 63.
[11] H.L. Gruber, J. Phys. Chem. 66 (1962) 48.
[12] S.J. Tauster, Acc. Chem. Res. 20(11) (1987) 389.
[13] T.P. Kobylinski, C.L. Kibby, R.B. Pannell and E.L. Eddy, U.S. Patent 4,605,676 (1986).
[14] E. Iglesia, S.L. Soled, R.A. Fiato and G.H. Via, J. Catal. 143 (1993) 345.
[15] D. Schanke, A.M. Hilmen, E. Bergene, K. Kinnari, E. Rytter and A. Holmen, Energy Fuels 10 (1996) 867.
[16] B.G. Johnson, M. Rameswaran, M.D. Patil, G. Muralidhar and C.H. Bartholomew, Catal. Today 6 (1989) 81.
[17] S. Soled and G.B. McVicker, Catal. Today 14 (1992) 189.
[18] D.E. Resasco and G.L. Haller, J. Catal. 82 (1983) 279.
[19] E. Iglesia, S.L. Soled, J.E. Baumgartner and S.C. Reyes, J. Catal. 153 (1995) 108.